Earth and Planetary Science Letters 481 (2018) 162–170

Contents lists available at ScienceDirect

Earth and Planetary Science Letters

www.elsevier.com/locate/epsl

Sedimentary evidence for enhanced hydrological cycling in response to rapid carbon release during the early Toarcian oceanic anoxic event

Kentaro Izumi[a,*], David B. Kemp[b], Shoma Itamiya[c], Mutsuko Inui[c]

[a] *Faculty & Graduate School of Education, Chiba University, 1-33 Yayoi-cho, Inage-ku, Chiba-shi, Chiba 263-8522, Japan*
[b] *School of Geosciences, University of Aberdeen, Old Aberdeen, Aberdeen, AB24 3UE, UK*
[c] *School of Science and Engineering, Kokushikan University, 4-28-1 Setagaya, Setagaya-ku, Tokyo 154-8515, Japan*

ARTICLE INFO

Article history:
Received 4 July 2017
Received in revised form 10 October 2017
Accepted 13 October 2017
Available online xxxx
Editor: D. Vance

Keywords:
Toarcian
carbon isotope
hydrological cycling
sedimentology
atmospheric warming

ABSTRACT

A pronounced excursion in the carbon-isotope composition of biospheric carbon and coeval seawater warming during the early Toarcian (∼183 Ma) has been linked to the large-scale transfer of ^{12}C-enriched carbon to the oceans and atmosphere. A European bias in the distribution of available data means that the precise pattern, tempo and global expression of this carbon cycle perturbation, and the associated environmental responses, remain uncertain. Here, we present a new cm-scale terrestrial-dominated carbon-isotope record through an expanded lower Toarcian section from Japan that displays a negative excursion pattern similar to marine and terrestrial carbon-isotope records documented from Europe. These new data suggest that ^{12}C-enriched carbon was added to the biosphere in at least one rapid, millennial-scale pulse. Sedimentological analysis indicates a close association between the carbon-isotope excursion and high-energy sediment transport and enhanced fluvial discharge. Together, these data support the hypothesis that a sudden strengthening of the global hydrological cycle occurred in direct and immediate response to rapid carbon release and atmospheric warming.

1. Introduction

The widespread occurrence of organic-rich facies deposited under reducing conditions during the early Toarcian has led to the recognition of one of the most pronounced oceanic anoxic events (OAEs) of the Phanerozoic. Broadly contemporaneous with deoxygenation is evidence for abrupt warming (Bailey et al., 2003), an increase in continental chemical weathering rates (Brazier et al., 2015; Cohen et al., 2004; Percival et al., 2016; Them et al., 2017a), and changes in atmospheric $p\mathrm{CO}_2$ (McElwain et al., 2005). The major sedimentary reservoirs of carbon at this time record a 3–7‰ negative excursion in carbon-isotopes (δ^{13}C), indicative of a large input of ^{12}C-enriched carbon (Hesselbo et al., 2000; Kemp et al., 2005; Svensen et al., 2007). Carbon-isotope records from Boreal and Tethyan sections often show that the overall shift to minimum values was stepped, comprising at least two rapid negative shifts in δ^{13}C superimposed on a more protracted decrease (e.g. Bodin et al., 2016; Hermoso et al., 2012; Hesselbo and Pienkowski, 2011; Jenkyns et al., 2001; Kemp et al., 2005; Ruebsam et al., 2014; Suan et al., 2015).

This δ^{13}C morphology has not yet been convincingly replicated outside of the Boreal and Tethyan realms, although recent work by Them et al. (2017b) indicates evidence for a complex and possibly stepped structure to the onset of the excursion in North America (Eastern Panthalassa Ocean). Establishing the precise pattern, reproducibility and magnitude of the early Toarcian δ^{13}C excursion is of central importance for determining the ultimate cause(s) of the event and associated environmental change. Similarly, there is a lack of data elucidating the environmental responses to inferred carbon release from globally distributed settings. These issues limit our understanding of the effects (both local and global) of carbon-forced greenhouse warming, and hence the role that events like the early Toarcian can play as analogues for modern day C release scenarios. To address these issues, we have conducted a high-resolution organic carbon-isotope and sedimentological analysis of an expanded lower Toarcian succession from Japan that was deposited at the margin of the Panthalassa Ocean (Fig. 1).

2. Geological setting

Lower Toarcian organic-rich mudstones, siltstones and fine-grained sandstones of the Nishinakayama Formation (Toyora Group) crop out in the Toyora area of southwest Japan, Yamaguchi prefecture (Fig. 1). The rocks form part of the fill of the Tabe Basin.

---

[*] Corresponding author.
E-mail address: izumi@chiba-u.jp (K. Izumi).

https://doi.org/10.1016/j.epsl.2017.10.030

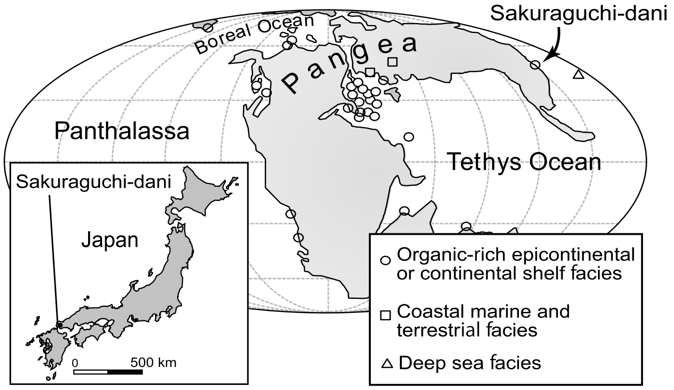

Fig. 1. Palaeogeography of the Early Jurassic and locations of lower Toarcian deposits. Note the European bias in study locations. Inset, location map of the Sakuraguchi-dani stream valley succession in Yamaguchi Prefecture, Japan. Sakuraguchi-dani location map and palaeogeographic reconstruction redrawn from Cohen et al. (2004) and Kemp and Izumi (2014).

A long history of research on the Sakuraguchi-dani stream bed succession (34°08′N 131°03′E; Fig. 1) has revealed a rich ammonite fauna, allowing demarcation of the lower Toarcian (Nakada and Matsuoka, 2011 and references therein). Recent geochemical analysis of the succession has demonstrated that the early Toarcian carbon cycle perturbation is well expressed, with a ∼3‰ negative excursion recorded in organic carbon-isotopes spanning ∼30 m (Izumi et al., 2012; Kemp and Izumi, 2014).

3. Analytical methods

3.1. Carbon isotope analysis

For this study, 80 mudstone samples were collected, primarily across the ∼5 m interval comprising the onset of the excursion, and analysed for the δ^{13}C of organic carbon. In addition, δ^{13}C analysis was also carried out on 6 macrofossil wood samples. For mudstone and wood δ^{13}C measurements, powdered samples were decalcified in 3 M HCl (heated to 60 °C for 3 h in the case of wood samples to help remove pyrite) and then washed with deionised water until neutrality was reached. After drying, samples were weighed into tin capsules and analysed on a Europa Scientific 20/20 mass spectrometer (rock samples) or a Thermo Scientific MAT253 isotope ratio mass spectrometer (wood samples). Precision for both instruments was quantified via analysis of standards, and was better than 0.2‰.

3.2. Rock-Eval analysis

Organic matter was characterised by Rock-Eval pyrolysis of 5 mudstone samples. Rock-Eval pyrolysis was carried out on 5 powdered samples distributed through the succession using a Rock-Eval 6 apparatus (Vinci Technologies), run in ‘Basic Method’ mode (see Behar et al., 2001). Both the S1 and S2 signals were successively determined with flame ionisation detection. The S1 signal corresponds to the amount of free hydrocarbons volatilised for 3 min at 300 °C, and the S2 signal represents the amount of hydrocarbons generated from kerogen cracking between 300 and 650 °C with a heating rate of 25 °C per 1 min. The amount of CO_2 generated between 300 and 400 °C was determined as the S3 signal, with infrared detection. All parameters (S1, S2, and S3) are expressed in mg of hydrocarbons or CO_2 per gram of rock. T_{max} is the temperature at which the maximum hydrocarbon yield resulting from kerogen cracking occurs. Residual organic carbon contents of the pyrolysed samples were obtained by combustion in air from 300 to 650 °C, with a heating rate of 20 °C per 1 min. The CO_2 and CO resulting from this combustion was also determined with an infrared cell, and corresponds to peak S4CO_2 for CO_2 and peak S4CO for CO. By using these parameters with the S1 to S3 signals, the total organic carbon (TOC) content (wt.%) was calculated as the sum of pyrolysed and residual organic carbon. The hydrogen index (HI, mg HC/g TOC) and oxygen index (OI, mg CO_2/g TOC) were calculated as S2/TOC, and S3/TOC, respectively.

For the application of Rock-Eval pyrolysis to the Toarcian sediments with basic interpretations, see Röhl and Schmid-Röhl (2005) for instance.

3.3. Sedimentological analysis

The sedimentology of the entire succession was investigated based on thin-section study of 72 mudstone samples, and polished/cut surface study of 28 sandstone samples. All thin-section observations were carried out using a polarising microscope (BX-51, Olympus) at Kokushikan University. In this study, silt beds are defined as silty layers with internal silty laminae, whereas a silt lamina is the smallest macroscopic layer without internal layering. Silt lamina thicknesses were measured from thin-section scanned images (jpeg format), using ImageJ image-processing software. Thin-section scanned images were obtained using a film scanner (KFS-1400, Kenko film scanner) that is equipped with polarisers. For thickness measurement of individual silt laminae, only distinct and continuous silt laminae recognised in a scan image were used. In the case of silt lamina whose thickness changes horizontally, the maximum thickness was used. All individual thickness data obtained from the single thin-section scanned image were used when calculating average thickness. Measurements of silt bed thicknesses were carried out in the same way.

For sandstone sedimentological analysis, sandstone samples were cut perpendicular to bedding planes and polished if necessary. Such cut or polished surfaces were scanned using a flatbed image scanner (GT-X770, EPSON). For one sandstone sample (Sample ID: 2016-S1-SST5), grain-size analysis was conducted in order to investigate the detailed sedimentary features that are difficult to identify by naked-eye observation. Grain-size analysis was based on the method described in Yoshida et al. (1995), which performs measurements of long-axis diameters of monocrystalline quartz grains under thin-section observation. In this study, long-axis diameters of monocrystalline quartz grains were measured in ImageJ using 5 × 5 mm meshed jpeg images of thin-section photomicrographs.

4. Results

4.1. Carbon-isotope data and Rock-Eval analysis

Our cm-scale δ^{13}C analysis of mudstones across the interval comprising the onset of the excursion reveals a steady decrease of ∼0.7‰ over the lowermost ∼13 m of the succession, from ∼−24.8‰ to ∼−25.5‰ (Fig. 2). At −4.58 m in the section, a −2.3‰ shift in δ^{13}C occurs over 21 cm of strata (labelled A on Fig. 2; Table S1 in supplementary materials). This decrease straddles an 18 cm thick horizon of unconsolidated, poorly sorted (clay to pebble sized) mudstone fragments. This is interpreted as a fault breccia (Fig. 2), though the lateral extent of the outcrop (∼20 cm) and position within a stream bed prevents a fuller assessment. Ammonite biostratigraphy indicates an early Toarcian age for strata immediately below and above this inferred fault (*P. paltus* zone, Fig. 2). Above this decrease, δ^{13}C increases by ∼1‰ over the succeeding ∼2 m (Fig. 2). Between −2.59 and −2.33 m, there is a second, broadly defined decrease in δ^{13}C of −2.2‰ (Fig. 2). This second decrease is interrupted by a positive excursion of ∼2.3‰